Regular Article

Surface-enhanced Raman spectroscopy for madder lake detection in painting layers

S. Innocenti[1,a] (ID), **M. Ricci**[2,b] (ID), **D. Quintero Balbas**[1] (ID), **R. Fontana**[1] (ID), **J. Striova**[1] (ID), **M. Becucci**[2] (ID)

[1] CNR-INO National Research Council, National Institute of Optics, Largo E. Fermi 6, 50125 Florence, Italy
[2] Department of Chemistry 'Ugo Schiff', University of Florence, via della Lastruccia 3-13, Sesto Fiorentino, 50019 Florence, Italy

Abstract Madder lake is the most utilized anthraquinone dyestuff in artworks. Its main constituents (alizarin and purpurin, together with other natural dyes) form an organometallic complex (the lake) insoluble in water by precipitation or adsorption of the dye onto an inorganic substrate. Raman spectra of madder lake are strongly affected by fluorescence, making its identification by Raman spectroscopy difficult or impossible. In this work, we prepared different lakes according to historical recipes and characterized them with X-ray diffraction (XRD), IR, and UV-Visible spectroscopies. Additionally, painting mock-ups were prepared and the lakes were extracted with hydrated and ethanol-rich agar gel beads. This work is aimed at showing the advantages and limits for the identification of the madder lake constituents by Raman and SERS (Surface-Enhanced Raman Spectroscopy) methods in the hydrogels used for sample micro-extraction. The main advantage of SERS for madder lake detection is to allow the user to acquire spectra in random spots in the gel bead, without the need for recrystallized grain localization in the dried hydrogel.

1 Introduction

Red lakes are colored inorganic–organic hybrid materials consisting of a water-insoluble organometallic complex formed by metal ions (for example Al^{3+}) linked to a specific functional group of the dye molecule. Their use in the production of artworks dates back to ancient times: they were prepared from natural dyes extracted from different varieties of plants' roots, from scale insects or inorganic substrates [1–3].

Among the red lakes, madder lake belongs to one of the oldest and the most important group of red dyestuffs, anthraquinones, extracted from the roots of *Rubia tinctorum L*. The main coloring compounds in madder are hydroxyanthraquinones, alizarin (1,2-dihydroxyanthraquinone, C.I. 75330) and purpurin (1,2,4-Trihydroxyanthraquinone, C.I. 58205). In classical antiquity, the most common substrate for the production of lake pigments was potash alum, a hydrated potassium aluminum sulfate ($KAl(SO_4)_2 \cdot 12H_2O$). An alkaline compound, such as potash (K_2CO_3) or lime ($Ca(OH)_2$), was often added to facilitate the reaction and enable the chelation of the dyestuff molecule to the aluminum cation.

In the literature, several studies report the way the dye sources and other substances involved in madder lake preparation, such as substrates and metal salts, may affect the color, the spectral properties [4, 5], and the lightfastness [6] of the final product.

Nevertheless, the structure of the metal-dye complexes that pure alizarin or purpurin produce within the lake and the nature of their established chemical interactions are still a matter of controversy. All the proposed structures refer to samples prepared in organic or mixed solvents or to purified lakes; therefore, the metal-dye systems can be different from those of the lakes obtained according to historical recipes using water and an excess of Al(III) [7–13].

The necessity of non-invasive and non-destructive methodologies for the study of cultural heritage is of fundamental importance for the preservation and conservation of artworks. In much-published research, lake pigments are simply recognized based on their fluorescence but cannot be easily discriminated [14]. Raman spectroscopy is routinely used for the non-destructive analysis of pigments and numerous case studies demonstrate its strength for the determination of both inorganic and organic materials in paint samples [15–17]. Often the direct Raman analysis of red lakes in paint samples or paintings is compromised by the strong fluorescence of the pigment which masks the Raman signal [18]. The interaction of the dye molecules with a nanostructured metal surface can strongly enhance the signal in Raman experiments as well as quench the fluorescence signal. For these reasons, surface-enhanced Raman spectroscopy (SERS) [19–22] has gained significant popularity as an alternative method for the analysis of red lake pigments. SERS (like chromatography methods [23]) is based on the extraction of dyes from micro-samples and on the subsequent interaction of the extracted molecules with nanostructured substrates for the detection of an enhanced Raman signal [24–29]. Methods based on SERS extraction of dyes in gels were presented, among the others, by Leona et al. [30] where methacrylate hydrogel and a water

[a] e-mail: silvia.innocenti@ino.cnr.it (corresponding author)

[b] e-mail: marilena.ricci@unifi.it (corresponding author)

solution of dimethylformamide (DMF) with disodium ethylenediaminetetraacetic acid (EDTA) were used to extract trace amounts of the target colorant from the substrate, or by Doherty et al. [25] that used methylcellulose for the formation of a gel, or even, Lofrumento et al. [26] that employed a SERS probe made of agar–agar added by silver colloid for a non-destructive and minimally invasive micro-extraction of dyes from textiles. SERS spectra can be directly measured on cross-sections following sample treatment [31] or laser ablation micro-sampling [32]. A general problem with the extraction of dyes from lake pigments—whether for SERS or chromatography—is that the information regarding the coordination of the dye molecules is lost. Also, the analysis and interpretation of these spectra is quite difficult and theoretical models could provide guidelines for the interpretation of the experimental results [33, 34]. Ab initio or DFT modeling provide reliable results on the structural and vibrational properties of both simple isolated chromophores [35, 36] and their Ag complexes as SERS models [37] but the complex environment of a lake often not known nor easy to be identified and represented in a theoretical approach [33].

We are working to improve the characterization of the lakes with micro-invasive methodologies coupled with Raman/SERS spectroscopy. Our recent work has proved how madder and cochineal lakes can be detected in painting layers with Raman spectroscopy in favorable conditions [38]. The employed process consists of the partial solubilization and recrystallization of the lakes in a hydrated, ethanol (EtOH)-rich, agar gel matrix. The solvents help the migration of the soluble fraction of the lake into the gel matrix and, once evaporated, micro grains are possibly formed inside the gel. The grains obtained from madder lake samples, after being analyzed by Raman spectroscopy, show the characteristic Raman spectra of the alizarin lake.

In this paper, we present a more detailed study of madder lake by Raman and SERS spectroscopy. The effect of EtOH on the samples of both natural madder lake and synthetic alizarin and purpurin lakes prepared according to historic recipes was verified either on lake powders and painting models prepared in the laboratory. Different analytical techniques were employed to complement the spectroscopic results from extracted samples. XRD, IR, and UV-Vis spectroscopies have been exploited to obtain information about the crystallinity of the formed lakes, the relative dyes components present in the powders, and the effective formations of the lakes, respectively. Finally, SERS experiments were carried out on the painting models both to improve sensitivity and, possibly, to simplify the sample analysis (i.e., to avoid the tedious search of small colored grains in the dried gel).

2 Materials and methods

2.1 Materials

Noble agar, Silver nitrate ($AgNO_3$) (purity $\geq$ 99.5%), sodium citrate dihydrate (ACS re-agent, $\geq$ 99.0%), alizarin (C.I. 75330) and purpurin (C.I. 58205) were purchased from Sigma-Aldrich. *Rubia tinctorum L.* roots were provided by Zecchi (Florence, Italy).

2.1.1 Lakes and mock-up preparation

The madder lake was prepared in-house from *Rubia Tinctorum L.* roots according to traditional recipes [39]. In particular, 2.5 g of roots were immersed in 50 ml of hot water and the obtained solutions, once filtered (pH 5–6), were brought to boiling and the alkaline pH was reached through the addition of a KOH water solution (1.4 g KOH in 50 ml water). Then, a rock alum solution (6 g $(KAl(SO_4)_2 \cdot 12H_2O$ in 50 ml of water) was added under magnetic stirring to precipitate the lake. After 30 min mixing, the preparation was left at room conditions for 24 h, and then the lake powder was filtered on paper. This solid was repeatedly washed with deionized water and dried. Alizarin and purpurin lakes were obtained starting from the dyes: 0.15 g of the dye were added to 125 ml of hot water, the solution was stirred for 10 min, filtered to remove suspended particles, and the alkaline pH was reached through the addition KOH water solution (3.5 g of KOH in 125 ml of water solution) and finally the rock alum solution (16 g of $KAl(SO_4)_2 \cdot 12H_2O$ in 125 ml of water) was added under magnetic stirring. The solution, after being stirred for 30 min, was kept at rest for 24 h, and then filtered. The solid was repeatedly washed with water and dried. The mock-up, purposely designed to simulate a real painting, was made of a wooden support, a gypsum and animal glue preparation layer and a madder, alizarin or purpurin lakes paint layer dispersed in egg yolk binder (the ratio binder-colorant was 1:1) (Fig. 1).

2.1.2 Ag colloidal solution and SERS substrate preparations

The silver colloidal solution was prepared according to the Lee-Meisel procedure, starting from silver nitrate (50 ml, 10^{-3} M in H_2O) and using sodium citrate (1 ml, $3.4 \; 10^{-2}$ M in H_2O) as reducing agent [40]. The resulting silver nanoparticles (AgNPs) were characterized through their UV-Vis spectra. Extinction spectra were measured on sample solutions held in a 1 mm optical path quartz cuvette. The plasmonic band maximum of the AgNPs dispersion was found around 430 nm, with typical extinction 1.6 and FWHM $\sim$100 nm (data not shown). The resulting AgNPs colloidal dispersion had a pH value around 5.5.

UV-Vis and SERS measurements on reference powders of alizarin, purpurin and corresponding lakes were performed using their EtOH solutions. SERS was carried out following the dried drop method: equivalent volumes of the sample solution and AgNPs colloid were mixed, let to stand for 10 min, then a drop was deposited in a microscope glass and air dried before starting the experiment.

Fig. 1 Painting model with (starting from left) madder, alizarin and purpurin lakes layers, and (below) the corresponding lakes
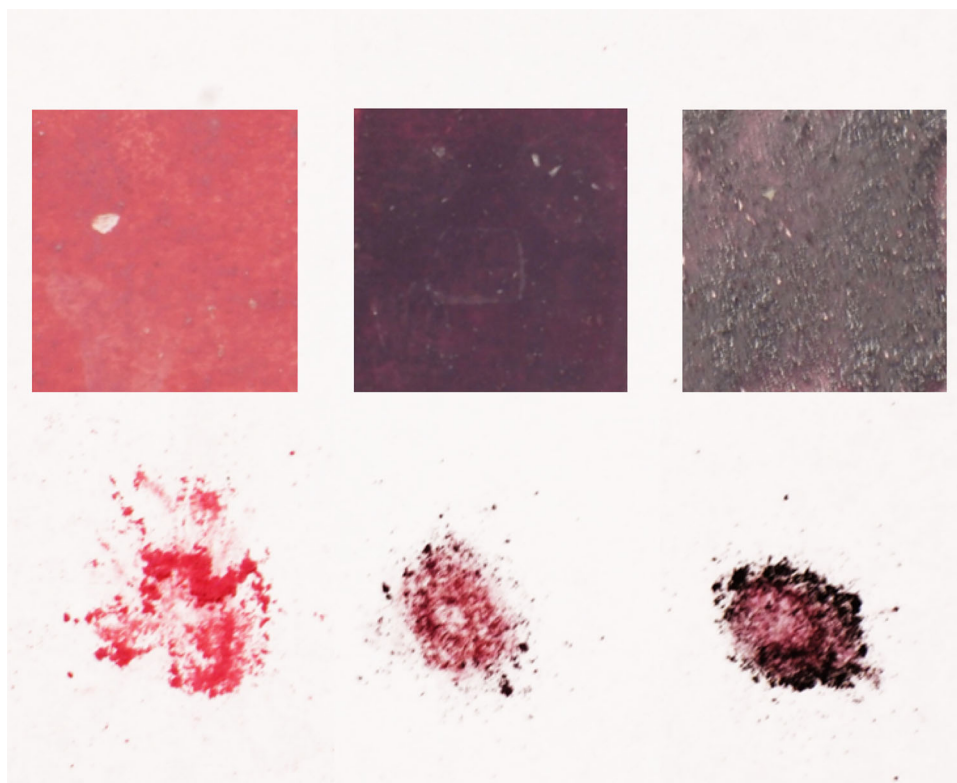
To prepare EtOH solution of the different materials and/or to recover their EtOH soluble fraction, a small amount of the sample (2 mg) was added to 1 ml of EtOH, the dispersion mixed in a Vortex mixer for 10 min, the EtOH solution recovered by filtration. For Raman measurements, the solvent evaporated and the resulting solid residue collected.

The agar gels were prepared as described in previous works [26, 41] by mixing 0.1 g of noble agar with 5 ml of water (for Raman experiments) or silver colloidal solution (for SERS experiments). The gel beads were loaded with 3 µl of EtOH to micro-extract soluble fraction of the coloring matter from the painted surfaces. We have tested different extraction times (5–30 min), and 5 min of contact time between the loaded gel bead and the painted surfaces were sufficient to obtain good results. To prepare for SERS measurements, the gel bead, after the extraction time, was further loaded with 3 µl of colloidal solution to improve sensitivity. Measurements started once the Ag-agar gel bead was completely dried.

2.2 Instrumentation

UV-Vis spectra were recorded with an Agilent Cary60 UV-Vis NIR spectrophotometer, with 2 nm resolution. UV-Vis-NIR Agilent Cary60 spectrometer (Agilent Technologies, Santa Clara, CA, USA).

The micro-Raman measurements were carried out with a Renishaw RM2000 spectrometer with a single-grating (1200 grooves/mm) and charge-coupled device (CCD with 577×400 pixels) air-cooled detector. The excitation source is a near infrared diode laser operating at 785 nm, a commonly used wavelength that allows to operate under a reduced fluorescence background and still provides a good Raman signal enhancement when the Lee-Meisel colloid is used for SERS due to the large bandwidth of the plasmonic band [22]. Laser beam focusing was accomplished through a $50 \times$ or $20 \times$ magnification objectives. The available laser power was up to 5 mW on the sample. Spectra were recorded with acquisition times in the order of 10 s, and spectral resolution of $4 \, \text{cm}^{-1}$. The spectrometer was routinely calibrated with respect to the $520 \, \text{cm}^{-1}$ band of a silicon wafer.

Diffraction patterns were recorded with an X-ray powder diffractometer X' Pert PRO (PANalytical) equipped with an ultrafast X'Celerator Real Time Multiple Strip (RTMS) detector with the following operative conditions: anticathode Cu ($\lambda = 1.5405$ Å), explored 2θ range between 3 and 70°, step size 0.04°, time to step 50 s.

Fourier transform infrared (FTIR) spectroscopy was performed on the powders using a Spectrum 100 Perkin Elmer with an attenuated total reflectance (ATR) diamond crystal. The detector is FR-DTGS (fast recovery deuterate L-alanine tryglycine sulfate) and the spectral range is 4000–$380 \, \text{cm}^{-1}$, with a spectral resolution of $4 \, \text{cm}^{-1}$.

Fig. 2 XRD diffraction patterns of
the different lakes. From
top-to-bottom: **a** alizarin lake,
b purpurin lake, **c** madder lake
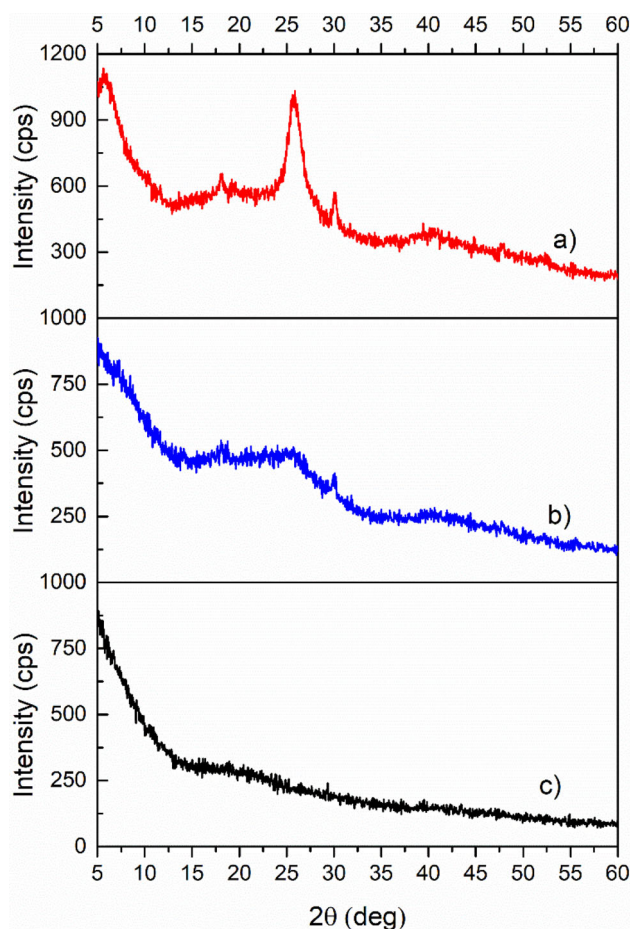
3 Results and discussion

3.1 Analysis of alizarin, purpurin and madder lakes

A first screening of the lakes was done by XRD diffraction to assess the degree of crystallinity of the materials and to verify the presence of unbound dyes. The experimental XRD patterns of alizarin and purpurin show some degree of crystallization (see Fig. SI1) while alizarin and purpurin lakes diffraction patterns (Fig. 2) exhibit limited resolved features (not detectable in case of madder lake). However, both for alizarin and purpurin lakes the resolved peaks are not associated to the free dyes (and we did not find a reasonable assignment for them from a database search). These lakes are prepared with non-stoichiometric recipes and in case of madder lake, prepared with a more traditional method, the excess of Al^{3+} ion is about 10 times larger than in the other cases (assuming a 0.1–1% dye content in the *Rubia tinctorum L*. roots). We associate the non-crystalline XRD signature of the madder lake to the larger amount of the inorganic phases present in this sample.

   Further insight on these materials was provided by their UV-Vis electronic absorption spectra (Fig. 3). Absorbance spectra of alizarin in EtOH are characterized by the absorption band at 430 nm ascribed to the free molecule in the neutral form. In case of alizarin lake, a band at 500 nm is present, as already reported for similar systems [42]. By fitting the spectra, it was possible to quantify the free alizarin in the alizarin lake as 2–3%, provided the extinction coefficient of both of them was known [43]. This result is compatible with the XRD evidence (no free dyes detected) given the limited sensitivity of XRD to the presence of minor components (about 4%, according to the instrumentation manufacturer). The UV-Vis spectra of purpurin and purpurin lake in EtOH show a similar trend. The purpurin spectrum corresponds to that of the neutral form, as reported by Grazia et al. [44] with three peaks at 455, 486 and 520 nm, while the purpurin lake spectrum shows bands at 508, 544, 578 nm. Given the limited solubility of the purpurin lake and the vibronic structure of the spectra, the same fitting procedure used to quantify the presence of free alizarin dye in its lake does not provide reliable results in this case. From the known extinction coefficients of both lakes, we made a rough estimate of the solubility of purpurin lake in EtOH as 6 times lower than that of the alizarin lake, i.e., approx. 6×10^{-6} M. The UV-Vis spectrum of the madder lake in EtOH solution was not measurable due to its limited solubility and lower dye content in the natural materials (plant roots).
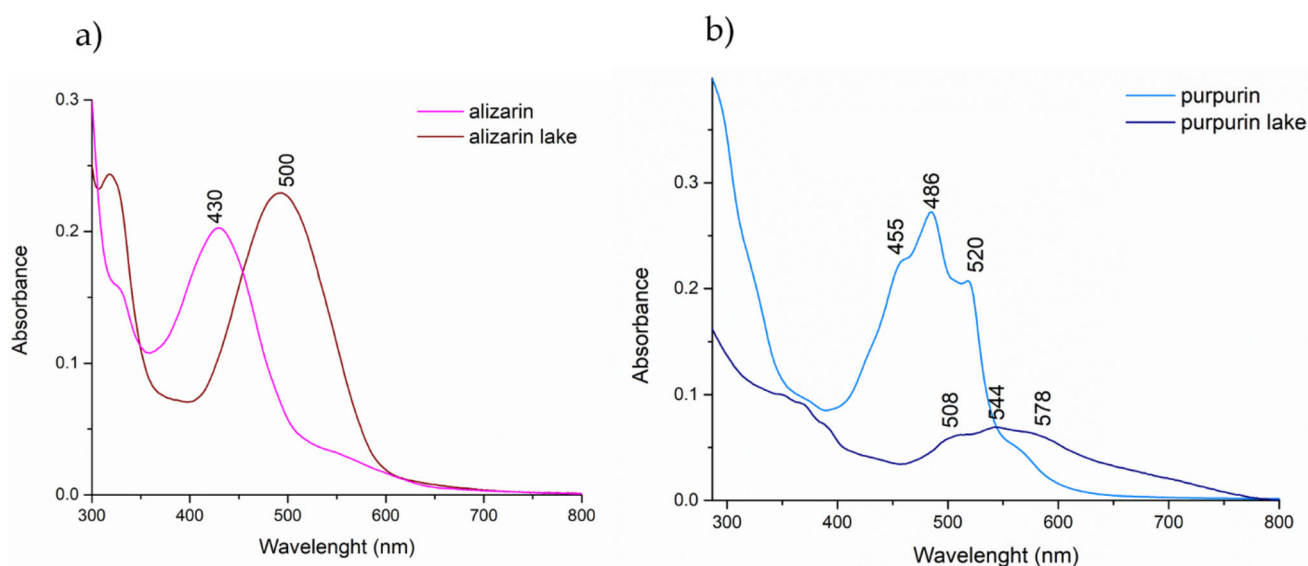
Fig. 3 a Absorption spectra of alizarin (pink line) and alizarin lake (red line) in ethanol, **b** purpurin (light blue line) and purpurin lake (blue line)

A more detailed characterization of these systems was provided by the IR and Raman spectra of the different lakes and the corresponding reference materials.

The FTIR spectra of alizarin and purpurin presented in Fig. 4 together with the corresponding lakes agree with previous reports [10, 13]. On the other hand, the madder lake FTIR spectrum (shown in Fig. SI2) is dominated by the inorganic substrate contribution. The spectra of the lakes' samples in Fig. 4 show lower intensity and some shifts in comparison with those of dyes. In fact, the bands referring to C=C, C=O, and C-O and O–H groups shifted significantly in the lakes spectra with respect to those of the reference materials. Following we discuss in more details some of the main spectral features for these systems. The bands referring to C=O groups (1662 and 1631 cm^{-1} in alizarin and 1668 and 1618 cm^{-1} in purpurin) merge to a single broad band/large shoulder in the lakes (1630 cm^{-1} in alizarin lake and purpurin lake), following the assignment in Ref. [13, 45–48]. The spectral region assigned to the C=C stretchings (1600–1400 cm^{-1} [13]) shows more bands in the lakes spectra. The analysis of other band systems is more reliable in case of the alizarin system which shows a simpler spectrum. The spectral region assigned to the OH bendings (1350–1300 cm^{-1} [47, 48]) shows a shift of the active bands for alizarin lake with respect to alizarin (1356 and 1328 from 1350 and 1327 cm^{-1}) while the band assigned to ν(C–O) shifted to 1285 from 1280 cm^{-1} [47]. Furthermore, the bands at 837 and 851 cm^{-1} observed in alizarin and purpurin lakes respectively, assigned to vibrations ν(Al-O) [49], show the formation of dye-Al^{3+} complexes. Also, the wide bands in the range 3000–3600 cm^{-1} and around 1630 cm^{-1} correspond to the stretching and bending vibrations of water molecules coordinating the Al^{3+} ion, while the bands associated to the vibrations ν(SO$_4^{2-}$) and δ(Al–OH) contribute to the broad band at 1090 cm^{-1}. Finally, it should be noticed that this 1090 cm^{-1} band dominates the madder lake mid-IR spectrum (see Fig. SI2).

Raman spectra of the different lakes from synthesis show a strong fluorescence background under the 785 nm excitation (see Fig. 5). However, the Raman spectrum of alizarin and purpurin lakes is still measurable (Fig. 5a, b) while that of madder lake in powder (Fig. 5c) is completely dominated by the intense background signal that completely covers the characteristic Raman bands (bands already observed under 1064 nm excitation [38]). The Raman spectra of the alizarin and purpurin lakes EtOH soluble fractions (solid recovered after solvent evaporation from the filtered solution obtained from partial solubilization of the lakes in EtOH, see paragraph 2.1.2) (Fig. 5 colored traces, Fig. SI3) have a much lower fluorescence background but present very similar Raman spectral features and relative intensities as the non-extracted lakes (Fig. 5 black traces). In case of alizarin lake, minor differences are observed in the EtOH soluble fraction: for example, the peak at 1453 cm^{-1} is a shoulder and the peaks at lower wavenumbers (e.g., 486 and 673 cm^{-1}) change their intensities. The Raman spectrum of alizarin lake agrees with previous experimental and theoretical reports [34, 38]. Raman spectra of purpurin lake, in both cases, are quite weak and characterized by broader bands, compatible with the crystallographic data which show an amorphous system.

The fraction of madder lake soluble in EtOH was characterized by Raman spectroscopy. To facilitate the comparison between the Raman and SERS datasets, we report a short summary in Table SI1 for alizarin and alizarin lake results. The measured madder lake Raman spectra (Fig. 5c) show some bands over a moderate fluorescence background and the experimental results can be classified as belonging to two different types, labelled here as type 1 and 2 (see also Fig. SI3 that contains a more thorough comparison of the different spectra, background subtracted). The type 1 Raman spectrum is very similar to that of synthetic alizarin lake (bands at 1472 (vs), 1453 (sh), 1358 (m), 1329 (s), 1297 (s), 1190 (m), 1160 (m) cm^{-1}). The assignment of this spectrum can tentatively follow the one provided for other alizarin-metal complexes [50], where it was suggested that the stronger Raman bands are enhanced by
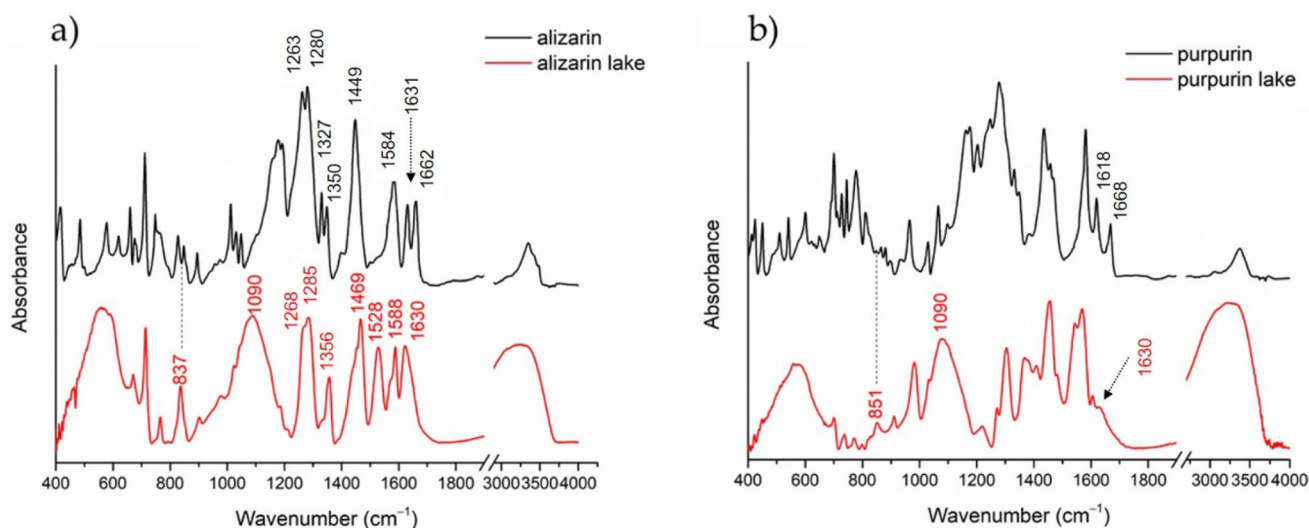
Fig. 4 ATR-FTIR spectra of **a** alizarin and alizarin lake; **b** purpurin and purpurin lake (intensity normalized for better visualization)
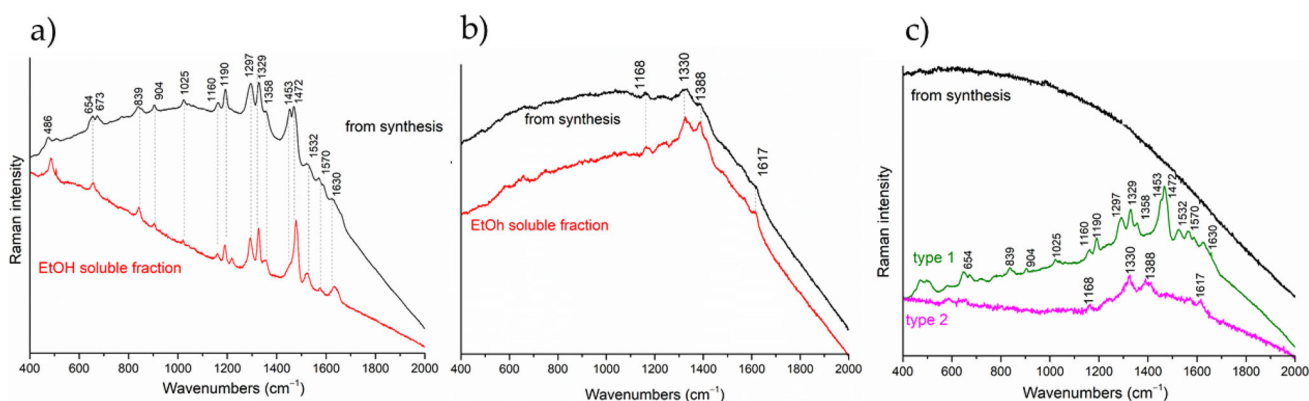

Fig. 5 Raman spectra of the lakes: **a** alizarin lake, **b** purpurin lake, and **c** madder lake: black traces are used for samples from synthesis and colors for samples recovered from EtOH-soluble lakes fraction after solvent evaporation (in case of madder lake we observed in different grains spectra associated either to alizarin or purpurine lakes (type 1 and 2, respectively). All spectra acquired with 785 nm excitation, 4 mW, 10 s, 5 accumulations

the higher electronic delocalization in metal bound alizarin. On the other hand, the type 2 Raman spectrum is dominated by broad bands at 1330 (s) and 1390 (vs) cm^{-1} characteristic of synthetic purpurin lake. Hence, it can be concluded that madder lake, when solubilized in EtOH and recovered by solvent evaporation, can lead to the formation of separated particles of alizarin and purpurin lakes.

We also measured the SERS spectra of alizarin and alizarin lake on dried drops of a solution made from 50 to 50% mixing of their EtOH solution (10^{-5} M) and the AgNPs colloid. The alizarin lake SERS spectra show different relative intensities in the bands for different sampling points and we categorize data into three main groups (Fig. 6), labelled as type 1–3. In all cases, the alizarin lake SERS spectra are rather similar but not equal to the SERS spectrum of alizarin and the presence of free alizarin is not evident. The SERS spectra of the alizarin lake show small but clearly discernable frequency shifts for different set of bands with respect to that of alizarin. The major changes are observed for the 1620 cm^{-1} band in the SERS spectra of alizarin, assigned as υ(C=O), that shifts to 1630 cm^{-1} in all SERS spectra of the lake, or the alizarin band system 1400–1460 cm^{-1}, due to υ(CC)/δ(COH)/δ(CH) vibrations, that upshifts by about 10 cm^{-1} in alizarin lake [36]. According to the different models proposed for the interaction mechanism of alizarin either with mordant ions or with AgNPs, the same alizarin functional groups are involved in the formation of both complexes. Therefore, similar Raman shifts could be expected for the SERS spectra of alizarin and for the Raman/SERS spectra of the alizarin lake with respect to pure alizarin Raman spectrum. Also, according to the present results (i.e. the SERS spectrum of the lake is different from that of alizarin), it can be safely assumed that the alizarin binding energy with the mordant ion is larger than with the AgNPs. Therefore, in case of alizarin lakes, it is plausible to hypothesize that SERS enhancement is promoted by a non-specific alizarin lake—AgNPs interaction driven by electromagnetic fields that could lead to small frequency shifts in the vibrational bands without major changes in the overall shape of the spectrum when comparing to the Raman spectrum of alizarin
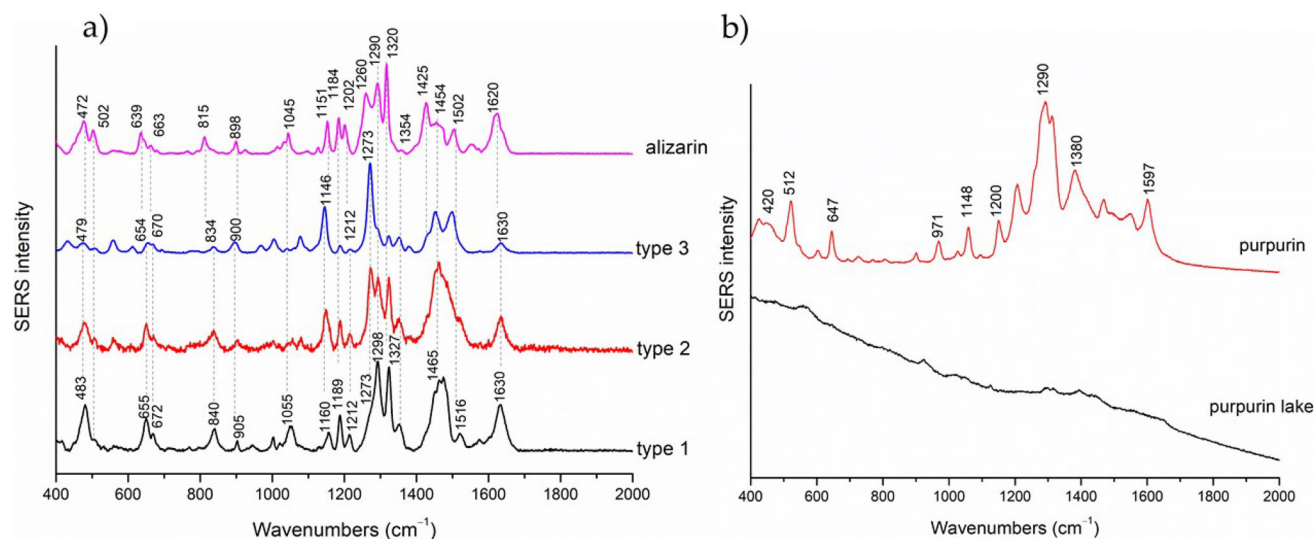
Fig. 6 SERS spectra of dried samples from EtOH solutions of: **a** alizarin and alizarin lake as obtained from different sampling points (0.5 mW laser power, 10 s integration time), bottom to top: alizarin lake (type 1, type 2 and type 3 spectra) and alizarin; **b** purpurin lake and purpurin (1.2 mW laser power, 10 s integration time) and purpurin. Alizarin and alizarin lake spectra are baseline subtracted, vertically shifted and intensity scaled

lake and the SERS spectrum of alizarin. Indeed, there is a striking similitude for the alizarin lake Raman spectrum shown in Fig. 5a and both the alizarin and alizarin lake (mostly type 1) SERS spectra shown in Fig. 6.

A simple data analysis on the SERS spectra of microextracted alizarin lake shows that spectra of type 2 are a linear combination (∼1:1) of the spectra type 1 and 3. Therefore, we hypothesize that at least two different kinds of supramolecular aggregates are present in the sample, associated either with different structures of the lake or different interaction motifs between the alizarin lake and the AgNPs. The present data could support the validation of structural models for this system (possibly developed in future work). Based on the current assignment of the alizarin Raman spectrum [36], we report significant changes in the SERS spectra of the alizarin lakes (type 1 and 3) associated with the vibrations involving different functional groups. The intense band at 1146 cm^{-1} in type 3 (υ(CC)/δ(CH)), became medium band at 1160 cm^{-1} in type 1 spectrum. The most intense band at 1273 cm^{-1} (υ(CO)/υ(CC)) in type 3 became a shoulder in type 1, but also the most intense bands at 1298 (υ(CO)/υ(CC)/δ(CCC)) and 1327 cm^{-1} (υ(CC)) in type 1 are weak bands in spectrum type 3. Also, the band at 1630 cm^{-1}, associated to the υ(C=O) stretching, is much stronger in type 1 than in type 3 spectra.

We proceeded similarly for purpurin and purpurin lake but we obtained different results with respect to the alizarin case (see Fig. 6b). While the purpurin SERS spectrum was easily observed, in agreement with previous results [26], the purpurin lake SERS spectrum was not easily discernible over the background Raman signals from the different ions present in the AgNPs colloid (e.g., citrate and nitrate ions). Possible reasons for the different results obtained in case of alizarin and purpurin lakes could be related to the very weak solubility purpurin lake in EtOH or to a different balance of supramolecular interactions in the colloidal matrix that limits the efficiency of the SERS process [51]. We did not observe either a clear SERS spectrum from EtOH extracted madder lake.

3.2 Analysis of mock-up samples

The results reported above on the study of the Raman/SERS spectra on samples recovered from EtOH solutions are the needed background information for the interpretation of data obtained by micro-extraction procedures from real or mock-up paintings. Indeed, the lakes' partial solubilization in EtOH is a reasonably good model for process that occurs when real or mock-up samples are undergoing micro-extraction by using a solvent loaded agar gel. Therefore, we proceed working on mock-up samples of paintings containing the lakes under study and applying the agar gel-based micro-extraction method described in previous work [38].

The efficiency of the micro-extraction process is well established and in some cases we have observed a partial recrystallization of the extract in the agar gel [38, 41]. Here we extend the work to mock-up samples prepared with madder, alizarin and purpurin lakes to establish the potentiality of both Raman and SERS spectroscopy for the identification of the different components in an artistic preparation.

In Fig. 7, Raman spectra acquired on grains formed in dried agar gels are reported. In the case of alizarin and purpurin lakes the Raman spectra correspond to those obtained on the powders recovered after solvent evaporation of the lake solutions in EtOH. However, it should be noticed that the much lower signal to noise ratio was observed for Raman spectra of the purpurin lake grains with respect to those of alizarin or madder lake samples, despite the higher laser power.

As regards the madder lake, the Raman spectra that we obtain in all the grains found in the dried agar gel are very similar to the Raman spectra of alizarin lake (characterized by sharp bands placed at 1472 (s), 1453 (sh), 1358 (m), 1329 (s), 1297 (s), 1190

Fig. 7 Raman spectra of grains in agar gel after micro-extraction from mock-ups and relative micro-photograph of gel matrix (right panels). Bottom-to-top: grains in madder lake mock-up extraction (0.5 mW laser power, 10 s integration time) and, as reference, alizarin lake (0.5 mW laser power, 10 s integration time) and purpurin lake (1.2 mW laser power, 10 s integration time)
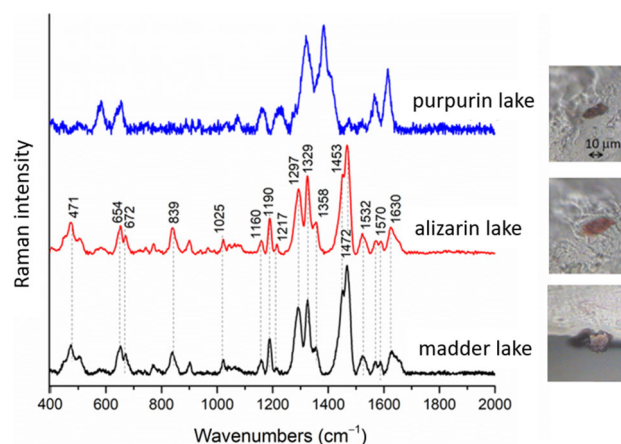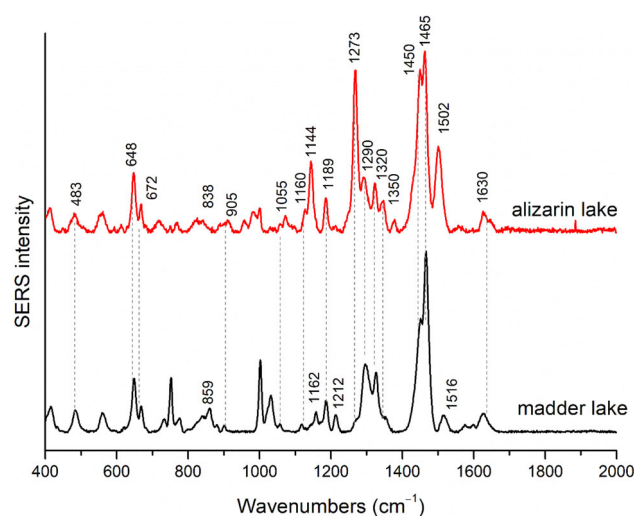

Fig. 8 SERS spectra from random spots in dried agar gel beads containing AgNPs used for ethanol aided micro-extraction of painting mock-ups prepared with alizarin lake or madder lake (0.5 mW laser power, 10 s, average of 10 measurements for each system). Spectra are baseline subtracted, vertically shifted and intensity scaled

(m), 1160 (m) cm^{-1}). It was not possible to detect Raman signals from micro-extracted madder lake associated with the presence purpurin lake, at least within the few grains observed in our experiments.

This is possibly related to the much lower EtOH solubility of purpurin lake with respect to the alizarin lake, as discussed in the analysis of the UV-Vis spectra, or to a higher affinity of purpurin lake to the agarose in the hydrogel (given the higher number of available OH groups with respect to the alizarin lake). The different signal to noise ratio observed for the micro-extracted mock-up containing pure alizarin or purpurin lakes is another possible limiting factor that should not be discounted.

We used an agar gel loaded with AgNPs to perform SERS experiments on the micro-extracted samples. The SERS spectra acquired on random spots in the dried bead (therefore skipping the long and tedious search of small grains of colored material that is needed for ordinary Raman measurement in this kind of samples) are shown in Fig. 8. SERS spectra of micro-extracted alizarin lake mock-ups show a spectral behavior similar to those obtained from evaporated EtOH solution of alizarin lake (shown in Fig. 7) and they can be taken as a linear combination (∼1:2) of the type 1 and 3 SERS spectra reported in Fig. 6. SERS spectra of micro-extracted purpurin lake mock-ups show very weak and broad bands, close to the background signal from the AgNPs colloid, in agreement with the results obtained on the EtOH soluble fraction of the purpurin lake. The SERS spectra of micro-extracted madder lake mock-ups show the characteristic SERS bands of alizarin lake (type 1) but the intensity pattern is quite different. It was not possible to identify the presence of the purpurin lake in the SERS spectra of micro-extracted madder lake. These SERS results agree with the Raman experiments on the micro-extracted samples from mock-up painting, showing only alizarin lake spectra. It should be noticed that while it was almost not possible to measure the SERS spectrum for the madder lake powder EtOH soluble fraction using the dried drop method, we succeed using micro-extraction with the agar gel. Possibly, as previously described [26, 52], the shrinking of the dried hydrogel improves the sensitivity of the SERS experiments due to the sample and nanoparticles concentration effect.

4 Conclusions

In this study we have investigated the structure and some chemical-physical properties of non-stoichiometric dye-Al^{3+} complexes deriving from the traditional lake preparation methods.

We report the SERS spectra of alizarin lake which can exhibit different patterns even in measurements made using the dried drop method. Therefore, we assume that at least two different kinds of supramolecular aggregates are present in the sample, associated with different crystal structures of the lake or different interaction motifs between the alizarin lake and the AgNPs. Instead, SERS spectra of purpurin lake are characterized by broad bands that are difficult to clearly disentangle from the background signals.

Raman spectra of madder lake are completely dominated by an intense fluorescence background which makes the lake identification difficult or impossible. In a previous report we have shown the possible formation of recrystallized painting materials in the hydrogel. They were possibly identified by a time-consuming search under microscopy observation and then possibly identified by Raman microscopy. Here we show how SERS technique gives information about the lake simply by repeating measurements in different random spots in the agar gel matrix, without the necessity of recrystallized grains into the gel. The proposed methodology is based on the use of an agar gel loaded with solutions of EtOH and AgNPs to enhance the Raman signal of the lake. This is a safe methodology for both the operator and the painting layers, and the minimal invasiveness of the agar gel was tested. We observed from the extracted madder lake in mock-up paintings a SERS spectrum that is associated with the alizarin lake, while the presence of the purpurin lake was not assessed.

UV-Vis spectroscopy was used to verify the formation of the lakes from the dyes (alizarin or purpurin) following a shift of the absorption maximum with respect to dyes, and to verify the solubility of the lakes. Alizarin lake has reasonable solubility in EtOH solution, about six times higher than purpurin lake. The higher solubility of alizarin lake in EtOH helps explain its higher detectability with respect to purpurin lake by Raman and SERS measurements on micro-extracted samples from the madder lake painting layers.

Data Availability Statement This manuscript has associated data in a data repository. [Authors' comment: Data are available on request.]

Declarations

Conflict of interest The authors declare no conflict of interest.

References

1. J. Kirby, Dye. Hist. Archeol. Text. **6**, 12 (1987)
2. J. Kirby, M. Spring, C. Higgitt, Natl. Gall. Tech. Bullettin **28**, 67 (2007)
3. J. Kirby, M.R. van Bommel, A. Verhecken, M. Spring, I. Vanden Berghe, H. Stege, M. Richter, Nat. Color. Dye. Lake Pigment. Pract. Recipes Their Hist. Sour. **1**, (2014)
4. J. Kirby, M. Spring, C. Higgitt, Natl. Gall. Tech. Bullettin **26**, 71 (2005)
5. C. Clementi, B. Doherty, P.L. Gentili, C. Miliani, A. Romani, B.G. Brunetti, A. Sgamellotti, Appl. Phys. A Mater. Sci. Process. **92**, 25 (2008)
6. C. Clementi, W. Nowik, A. Romani, F. Cibin, G. Favaro, Anal. Chim. Acta **596**, 46 (2007)
7. C.H Wunderlich, G. Bergerboff, Zeitschrift Für Krist.-Cryst. Mater. **207**, 185 (1993)
8. C.-H. Wunderlich, G. Bergerhoff, Chem. Ber. **127**, 1185 (1994)
9. P. Soubayrol, G. Dana, P.P. Man, Magn. Reson. Chem. **34**, 638 (1996)
10. E.G. Kiel, P.M. Heertjes, J. Soc. Dye Colour **79**, 186 (1963)
11. F.Y. Fain, B.E. Zaitsev, M.A. Ryabov, Rus. J. Coord. Chem. **30**, 365 (2004)
12. M. Doskocz, K. Kubas, A. Frackowiak, R. Gancarz, Polyhedron **28**, 2201 (2009)
13. G. Zhuang, S. Pedetti, Y. Bourlier, P. Jonnard, C. Méthivier, P. Walter, C.M. Pradier, M. Jaber, J. Phys. Chem. C **124**, 12370 (2020)

14. J. Seixas De Melo, A.P. Moura, M.J. Melo, J. Phys. Chem. A **108**, 6975 (2004)
15. I.M. Bell, R.J.H. Clark, P.J. Gibbs, Spectrochim. Acta Part A Mol. Biomol. Spectrosc. **53**, 2159 (1997)
16. F. Casadio, C. Daher, L. Bellot-Gurlet, Top. Curr. Chem. **374**, 62 (2016)
17. C.H. Lin, Y.F. Chang, Anal. Sci. **38**, 483 (2022)
18. I. Osticioli, A. Nevin, D. Anglos, A. Burnstock, S. Cather, M. Becucci, C. Fotakis, E. Castellucci, J. Raman Spectrosc. **39**, 307 (2008)
19. A.V. Whitney, R.P. Van Duyne, F. Casadio, J. Raman Spectrosc. **37**, 993 (2006)
20. F. Pozzi, M. Leona, J. Raman Spectrosc. **47**, 67 (2016)
21. C.L. Brosseau, K.S. Rayner, F. Casadio, C.M. Grzywacz, R.P. Van Duyne, Anal. Chem. **81**, 7443 (2009)
22. M. Ricci, E. Trombetta, E. Castellucci, M. Becucci, J. Raman Spectrosc. **49**, 997 (2018)
23. I. Degano, P. Tognotti, D. Kunzelman, F. Modugno, Herit. Sci. **5**, 1 (2017)
24. F. Pozzi, J.R. Lombardi, S. Bruni, M. Leona, Anal. Chem. **84**, 3751 (2012)
25. B. Doherty, B.G. Brunetti, A. Sgamellotti, C. Miliani, J. Raman Spectrosc. **42**, 1932 (2011)
26. C. Lofrumento, M. Ricci, E. Platania, M. Becucci, E. Castellucci, J. Raman Spectrosc. **44**, 47 (2013)
27. H.E. Mayhew, D.M. Fabian, S.A. Svoboda, K.L. Wustholz, Analyst **138**, 4493 (2013)
28. A. Cesaratto, M. Leona, F. Pozzi, Front. Chem. **7**, 105 (2019)
29. I. Marcaida, M. Maguregui, H. Morillas, C. García-Florentino, V. Pintus, T. Aguayo, M. Campos-Vallette, J.M. Madariaga, Anal. Bioanal. Chem. **409**, 2221 (2017)
30. M. Leona, P. Decuzzi, T.A. Kubic, G. Gates, J.R. Lombardi, Anal. Chem. **83**, 3990 (2011)
31. A. Idone, M. Aceto, E. Diana, L. Appolonia, M. Gulmini, J. Raman Spectrosc. **45**, 1127 (2014)
32. A. Cesaratto, M. Leona, J.R. Lombardi, D. Comelli, A. Nevin, P. Londero, Angewandte Chemie **126**, 14601 (2014)
33. L. Carta, M. Biczysko, J. Bloino, D. Licari, V. Barone, Phys. Chem. Chem. Phys **16**, 2897 (2014)
34. M. Pagliai, I. Osticioli, A. Nevin, S. Siano, G. Cardini, V. Schettino, J. Raman Spectrosc. **49**, 668 (2018)
35. C. Lofrumento, F. Arci, S. Carlesi, M. Ricci, E. Castellucci, M. Becucci, Spectrochim. Acta-Part A Mol. Biomol. Spectrosc. **137**, 677 (2015)
36. M.V. Cañamares, J.V. Garcia-Ramos, C. Domingo, S. Sanchez-Cortes, J. Raman Spectrosc. **35**, 921 (2004)
37. C. Lofrumento, E. Platania, M. Ricci, M. Becucci, E.M. Castellucci, J. Phys. Chem. C **120**, 12234 (2016)
38. S. Innocenti, M. Ricci, G. Lanterna, R. Fontana, J. Striova, M. Becucci, Eur. Phys. J. Plus **136**, 1 (2021)
39. M. Merrifield, *Original Treatises, Dating From The XIIth To The XVIIIth Centuries On The Arts Of Painting, In Oil, Miniature, Mosaic, And On Glass; Of Gilding, Dyeing, And The Preparation Of Colours And Artificial Gems* (John Murray, London, 1849)
40. P.C. Lee, D. Meisel, J. Phys. Chem. **86**, 3391 (1982)
41. E. Platania, C. Lofrumento, E. Lottini, E. Azzaro, M. Ricci, M. Becucci, Anal. Bioanal. Chem. **407**, 6505 (2015)
42. S. Say-Liang-Fat, J.P. Cornard, Polyhedron **30**, 2326 (2011)
43. A. Claro, M.J. Melo, S. Schäfer, J.S.S. de Melo, F. Pina, K.J. van den Berg, A. Burnstock, Talanta **74**, 922 (2008)
44. C. Grazia, C. Clementi, C. Miliani, A. Romani, Photochem. Photobiol. Sci. **10**, 1249 (2011)
45. E.G. Kiel, P.M. Heertjes, J. Soc. Dye. Colour. **79**, 21 (1963)
46. M. Koperska, T. Łojewski, J. Łojewska, Anal. Bioanal. Chem. 3271–3283 (2011)
47. L. Legan, K. Retko, P. Ropret, Microchem. J. **127**, 36 (2016)
48. E. Pérez, I.A. Ibarra, A. Guzmán, E. Lima, Spectrochim. Acta Part A Mol. Biomol. Spectrosc. **172**, 174 (2017)
49. H. Wijnja, C.P. Schulthess, Spectrochim. Acta-Part A Mol. Biomol. Spectrosc. **55**, 861 (1999)
50. S. Murcia-Mascarós, C. Domingo, S. Sanchez-Cortes, M.V. Cañamares, J.V. Garcia-Ramos, J. Raman Spectrosc. **36**, 420 (2005)
51. E. Roschi, C. Gellini, M. Ricci, S. Sanchez-Cortes, C. Focardi, B. Neri, J.C. Otero, I. López-Tocón, G. Smulevich, M. Becucci, Nanomaterials **11**, 881 (2021)
52. M. Fan, G.F.S. Andrade, A.G. Brolo, Anal. Chim. Acta **1097**, 1 (2020)